SAND2000-2037C

Characteristics of Novel InGaAsN Double Heterojunction Bipolar Transistors

N. Y. Li[1], P. C. Chang[2], A. G. Baca[2], J. R. Laroche[3], F. Ren[3], E. Armour[4], P. R. Sharps[1], and H. Q. Hou[1]

[1] Emcore PhotoVoltaics, Emcore Corp., 10420 Research Rd. SE, Albuquerque, NM 87123.
[2] Sandia National Laboratories, 1515 Eubank Blvd. SE, Albuquerque, NM 87185-0603.
[3] University of Florida, Department of Chemical Engineering, Gainesville, FL 32611.
[4] Emcore Corp., 394 Elizabeth Ave., Somerset, NJ 08873.

RECEIVED
SEP 15 2000
OSTI

Abstract

We demonstrate, for the first time, both functional Pnp AlGaAs/InGaAsN/GaAs (Pnp InGaAsN) and Npn InGaP/InGaAsN/GaAs (Npn InGaAsN) double heterojunction bipolar transistors (DHBTs) using a 1.2 eV $In_{0.03}Ga_{0.97}As_{0.99}N_{0.01}$ as the base layer for low-power electronic applications. The Pnp InGaAsN DHBT has a peak current gain (β) of 25 and a low turn-on voltage (V_{ON}) of 0.79 V. This low V_{ON} is ~0.25 V lower than in a comparable Pnp AlGaAs/GaAs HBT. For the Npn InGaAsN DHBT, it has a low V_{ON} of 0.81 V, which is 0.13 V lower than in an InGaP/GaAs HBT. A peak β of 7 with nearly ideal I-V characteristics has been demonstrated. Since GaAs is used as the collector of both Npn and Pnp InGaAsN DHBTs , the emitter-collector breakdown voltage (BV_{CEO}) are 10 and 12 V, respectively, consistent with the BV_{CEO} of Npn InGaP/GaAs and Pnp AlGaAs/GaAs HBTs of comparable collector thickness and doping level. All these results demonstrate the potential of InGaAsN DHBTs as an alternative for application in low-power electronics.

Introduction

Modern day portable electronics has lead to a lot of conveniences, and become part of everyday life. High performance and portability with longer battery lifetime has become much more critical. Low-power electronics promises longer battery lifetime, which is highly desirable. An HBT using a small bandgap energy (E_G) material in the base has lower turn-on voltage (V_{ON}), a highly desirable characteristic for reducing power dissipation in circuits. One approach uses strained InGaAs on GaAs; however, the range of In composition for growing strained InGaAs on GaAs without formation of misfit dislocations is very limited [1]. In addition, due to the compressive strain, the E_G of InGaAs increases, reducing the benefits of having InGaAs in the base layer. For this reason, most of the earlier works on low-power HBTs have focused on the InP/InGaAs

DISCLAIMER

This report was prepared as an account of work sponsored by an agency of the United States Government. Neither the United States Government nor any agency thereof, nor any of their employees, make any warranty, express or implied, or assumes any legal liability or responsibility for the accuracy, completeness, or usefulness of any information, apparatus, product, or process disclosed, or represents that its use would not infringe privately owned rights. Reference herein to any specific commercial product, process, or service by trade name, trademark, manufacturer, or otherwise does not necessarily constitute or imply its endorsement, recommendation, or favoring by the United States Government or any agency thereof. The views and opinions of authors expressed herein do not necessarily state or reflect those of the United States Government or any agency thereof.

DISCLAIMER

Portions of this document may be illegible in electronic image products. Images are produced from the best available original document.

material system. The InP technology, however, is relatively expensive compared to GaAs foundry technology, and thus its application has been limited.

InGaAsN is a new material system that has received a lot of attention lately. Incorporating a small amount of nitrogen (N) into InGaAs results in a reduction of its lattice constant, thus reducing the strain of InGaAs layer grown on GaAs [2,3]. In addition, due to a large bandgap bowing, the E_G decreases as N is added [4], a desirable characteristic for GaAs-based device structures that require material with a smaller E_G than the 1.42 eV of GaAs. Recent advances in the InGaAsN material system has led to much progress on the application of this material system for a variety of devices [5-7]. The InGaAsN material system may be an excellent alternative for low-power HBTs. Its small E_G allows lower V_{ON} and it is compatible with the existing GaAs foundry technology; thus, it is more likely to be used in inexpensive low-power electronics [8,9].

The band alignment of the InGaAsN material system is illustrated in Fig. 1. As N is incorporated into GaAs, a tensile strain develops and both the conduction band (E_C) and the valence band (E_V) are lowered. On the other hand, a compressive strain builds up as In is added into GaAs, the E_C is lowered, and the E_V is raised. By incorporating proper amount of In and N into GaAs simultaneously, InGaAsN lattice matched to GaAs can be obtained. The E_C of the resulting InGaAsN would be much lower than that of GaAs because of the aggregated lowering effect from the incorporation of N and In. The energy level of E_V would depend on the amount of N incorporation. For 1.2 eV $In_{0.03}Ga_{0.97}As_{0.99}N_{0.01}$, the effects of N and In incorporation on E_V are almost compensated, namely, the E_V is relatively unchanged compared to the E_V level of GaAs [10].

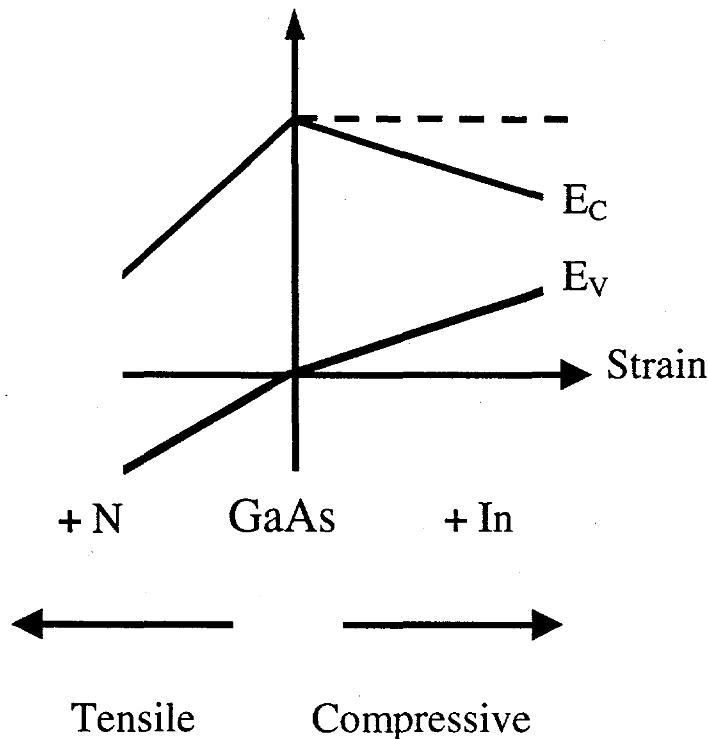

Figure 1 : Effects of N and In incorporation into GaAs on conduction band and valence band edges.

The resulting band alignment as shown in Fig. 2a, shows an unique band structure favorable for Pnp InGaAsN HBTs; a large conduction band discontinuity (ΔE_C) to suppress minority carrier electrons from being injected into the emitter, while a small valence band discontinuity (ΔE_V) facilitates holes transport from the emitter to the base.

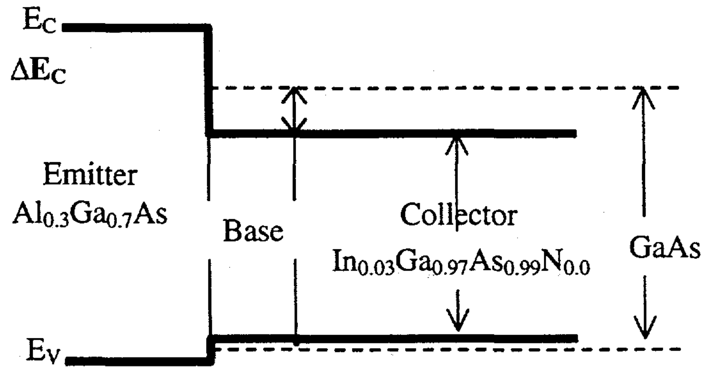

(a)

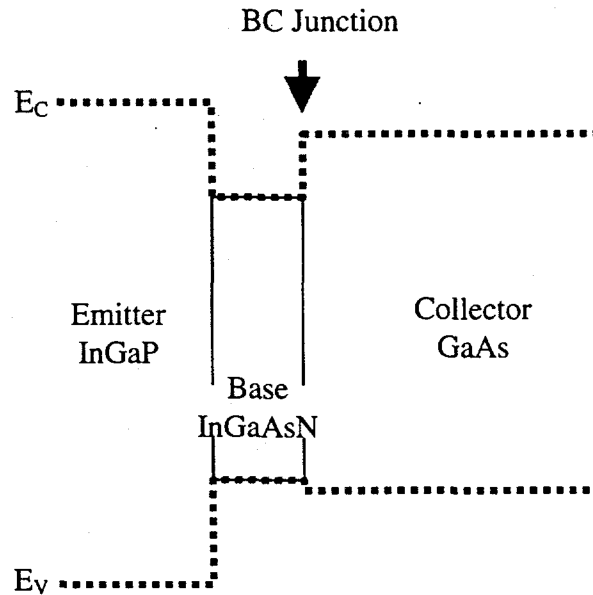

(b)

Figure 2 : (a) The band alignment of the Pnp $Al_{0.3}Ga_{0.7}As/In_{0.03}Ga_{0.97}As_{0.99}N_{0.01}$ DHBT compared to the Pnp $Al_{0.3}Ga_{0.7}As$/GaAs HBT
(b) The band alignment of the Npn InGaP/$In_{0.03}Ga_{0.97}As_{0.99}N_{0.01}$/GaAs DHBT.

However, Npn InGaAsN-based HBTs present a more difficult challenge. Contray to Pnp InGaAsN DHBTs, the significant ΔE_C at the p-InGaAsN/n-GaAs base-collector (B-

C) heterojunction shown in Fig. 2b is harmful for Npn InGaAsN DHBTs. Electrons are suppressed from being injected from base into the collector. To alleviate this effect, a thin 300Å-thick $In_xGa_{1-x}As$ graded layer (x linearly graded from 0 to 0.2) with δ-doping located close to B-C junction is introduced and compared against an abrupt Npn InGaAsN DHBT. In addition, undoped OMVPE-grown InGaAsN usually is p-type with a background concentration of $1\text{-}2\times10^{17}$ cm^{-3}, making it difficult to grow a high-quality lightly-doped n-type InGaAsN epilayer with a carrier concentration of $n=1\text{-}3\times10^{16}$ cm^{-3} for single heterojunction HBTs. Therefore, in this work, an n-type GaAs was chosen as the collector of Npn InGaAsN DHBTs.

Experimental procedures

The Pnp and Npn InGaAsN DHBTs were grown by an Emcore D180 turbodisk reactor. Trimethylindium, trimethylgallium, 100% arsine (AsH_3), and 1,1-dimethylhydrazine (DMHy) were used as the In, Ga, As, and N precursors, respectively, for the growth of 1.2 eV $In_{0.03}Ga_{0.97}As_{0.99}N_{0.01}$ base layer. The flow rate ratio of DMHy/(DMHy+AsH_3) was fixed at 0.95. The In and N compositions were determined by secondary ion mass spectroscopy and high-resolution x-ray diffraction measurements. The doping concentrations in epilayers were confirmed with Polaron and Hall measurements. The DHBT devices were fabricated using a triple mesa process. Selective wet etching was used to expose the base and the subcollector surface, as well as for achieving device isolation. The AlGaAs, GaAs and InGaAsN etches were done using the 1 H_3PO_4 : 4 H_2O_2 : 45 H_2O solution, while a diluted HCl solution was used to etch the InGaP emitter layer. For Npn InGaAsN DHBTs, Pd/Ge/Au annealed at 175°C for 1 hour was used for the emitter and collector contact metal [11]. Non-alloyed Pt/Ti/Pt/Au was used for the p-type base. For Pnp InGaAsN DHBTs, Pt/Ti/Pt/Au formed non-alloyed ohmic contacts for the emitter and the collector, and Pd/Ge/Au was used for the base contact metal. For this work, the devices were not passivated. DC characteristics of InGaAsN DHBTs were tested using an HP-4145 Semiconductor Parameter Analyzer.

Results & discussions

(a) Pnp InGaAsN DHBTs

The structure of the Pnp InGaAsN DHBT is shown in Table 1. The resulting band structure resembles the diagram shown in Fig. 2a. For the $Al_{0.3}Ga_{0.7}As/In_{0.03}Ga_{0.97}As_{0.99}N_{0.01}$ emitter-base (E-B) junction, the ΔE_V at the base emitter junction would be around 0.15 eV, while the ΔE_C would be more than 0.5 eV. At the B-C junction, the ΔE_V between $In_{0.03}Ga_{0.97}As_{0.99}N_{0.01}$ and GaAs is negligible. As discussed earlier, this kind of bandgap alignment is favorable for Pnp DHBT applications. Thus, GaAs can be used instead of InGaAsN in the collector without typical penalties suffered by DHBTs. At the same time, taking advantage of the larger E_G of GaAs, which allows for higher breakdown voltages, especially when compared to other low-power HBTs based on InP/InGaAs material system. In addition, the hole mobility (μ_p) of the best 1.2 eV InGaAsN reported to date is about half of the μ_p typically

observed in GaAs, therefore using GaAs as the collector material would affect the rf performance of this device positively.

InGaAsN Pnp HBT	Material	Thickness	Doping [cm^{-3}]
Emitter	p^+ GaAs	20	2.00E+19
	p $Al_{0.}$ GaAs	10	3.00E+18
	p $Al_{0.}$ GaAs	5	*undoped*
Base Layer	n InGaAsN	10	3.00E+18
Collector	p^- GaAs	50	3.00E+16
Subcollector	p^+ GaAs	50	2.00E+19
Substrate	S. I.		

Table 1: The layer structure of the Pnp $Al_{0.3}Ga_{0.7}As/In_{0.03}Ga_{0.97}As_{0.99}N_{0.01}/GaAs$ DHBT.

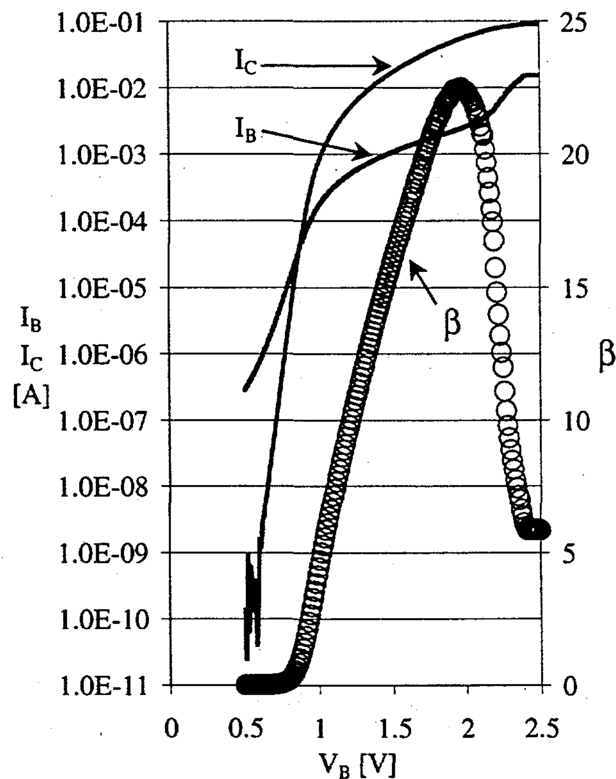

Figure 3 : The Gummel plot of the Pnp $Al_{0.3}Ga_{0.7}As/In_{0.03}Ga_{0.97}As_{0.99}N_{0.01}$ DHBT.

The Gummel plot and the measured common-emitter (CE) current-voltage (IV) plot are shown in Fig. 3 and Fig. 4, respectively. As shown in Fig. 3, the InGaAsN DHBT has a peak current gain (β) of 25, which is sufficient to be used for many circuit applications. More importantly, the V_{ON} of the InGaAsN DHBT, as defined by the base-emitter junction bias (V_{BE}) at which the collector current (I_C) exceeds 1.0 μA, is only 0.79 V,

~0.26 V lower than the 1.03 V measured in an $Al_{0.3}Ga_{0.7}As/GaAs$ HBT with a similar structure, confirming that HBTs with an InGaAsN base layer can be used as an alternate approach for reducing power dissipation in a low-power circuit. Also, because GaAs is used for the collector layer, the emitter collector breakdown voltage (BV_{CEO}) is about 12 V, comparable to the BV_{CEO} observed in an AlGaAs/GaAs HBT with similar collector thickness and doping level. Other important parameters considered are the offset voltage (V_{offset}) and the saturation voltage (V_{sat}). As shown in Fig. 4, the V_{offset} of our device is about 220 mV, which is slightly higher than what is measured in an AlGaAs/GaAs HBT. The V_{sat} is also slightly higher than expected, ranging from 0.55 V to 0.85 V for I_C ranging from about 1.4 mA to 12.0 mA. This discrepancy is due to the material quality of the $In_{0.03}Ga_{0.97}As_{0.99}N_{0.01}$ being not as good as that of the GaAs yet. The base sheet resistance (R_B) of the n-type $In_{0.03}Ga_{0.97}As_{0.99}N_{0.01}$ base layer is about 3 KΩ/Square. This high R_B is mainly arised from a much lower electron mobility (μ_n) of 350 cm^2/Vs in the base layer ($n=3x10^{18}$ cm^{-3}) than that of ~2000 cm^2/Vs in GaAs, leading to the high V_{offset} and high V_{sat} as observed in Fig. 4.

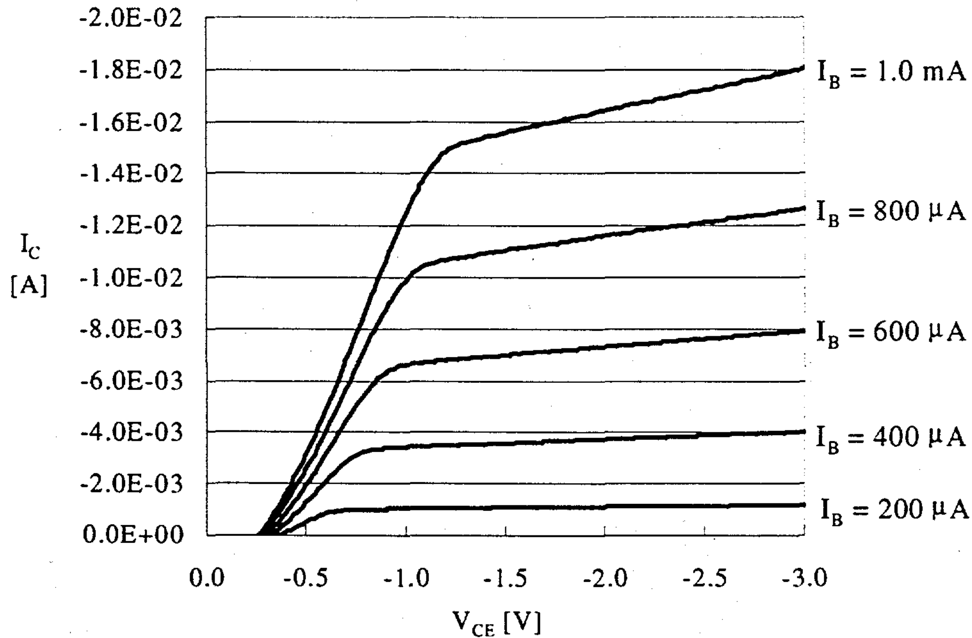

Figure 4 : The common-emitter IV plot of the Pnp $Al_{0.3}Ga_{0.7}As/In_{0.03}Ga_{0.97}As_{0.99}N_{0.01}$ DHBT.

In addition, the β for a typical $Al_{0.3}Ga_{0.7}As/GaAs$ Pnp HBT is greater than 100. Considering the presence of a larger ΔE_C at the $Al_{0.3}Ga_{0.7}As/In_{0.03}Ga_{0.97}As_{0.99}N_{0.01}$ B-E junction, and the fact that β should increase exponentially with increasing ΔE_C, β should ideally be greater than 25. A possible cause may be the presence of recombination centers in the $In_{0.03}Ga_{0.97}As_{0.99}N_{0.01}$ base, thus resulting in high levels of recombination current and lower β. One indication that the material could be improved is the high

ideality factor of the base current (n_{Ib}). A high n_{Ib} indicates high level of recombination current, thus reducing the value of β. However, as shown in Fig. 3, the n_{Ib} is very large (about 3.2), indicating that there is more than just intrinsic base recombination effects. Since the device tested has not been passivated, a possible source of recombination current is the surface recombination.

(b) Npn InGaAsN DHBTs

	Material	Thickness [Å]	Doping [cm^{-3}]
Contact cap layer	n^+ $In_{0.53}GaAs$	300	2.00E+19
Graded contact layer	n^+ $In_{0-0.53}GaAs$	300	2.00E+19
Subemitter	n^+ GaAs	1000	2.00E+18
Emitter	*n* InGaP	500	2.00E+17
Base Layer	*p*- InGaAsN	700	1.00E+19
Space Layer	*undoped* InGaAsN	50	*undoped*
Graded collector	n^- $In_{0-0.1}GaAs$	300	3.00E+16
Collector	n^- GaAs	5000	3.00E+16
Subcollector Layer	n^+ GaAs	5000	5.00E+18
Substrate		S. I. GaAs	

Table 2: The layer structure of Npn InGaP/InGaAsN/GaAs DHBTs

Table 2 illustrates the layer structure of emitter-up Npn InGaAsN DHBTs with and without an $In_xGa_{1-x}As$ graded layer. Large-area 100x100 μm^2 DHBT devices were examined for DC performance. The effect of V_{BC} on β for abrupt and graded B-C junctions at a V_{BE} of 2.3 volt is shown in Fig. 5. β is less than one when V_{BC} is lower than 1.2 volt for both abrupt and graded InGaP/InGaAsN DHBTs. When V_{BC} is higher than 1.2 volt, β is increased linearly with increasing V_{BC}, and a higher β was obtained for the graded B-C junction DHBT. The peak β for an abrupt and a graded B-C junction DHBTs are 3.4 and 4.3, respectively, at a V_{BC} of 9 volt. These results illustrate how the current blocking effect due to ΔE_c barrier at the B-C junction limits β. A typical Gummel plot of graded B-C junction InGaP/InGaAsN DHBTs with V_{BC}=9 volt is shown in Fig. 6. It is clearly observed that I_C is always higher than I_B when V_{BE} is higher than 0.5 volt. The V_{on} of an Npn InGaAsN DHBT at I_c in the range of 1 μA to 1mA is approximately 0.05 V lower than that of an InGaP/GaAs HBT with a similar structure. This value is ~ 0.17 volt higher than our expectations, mainly due to an abrupt B-E junction was used. A peak β of 5.3 has been achieved at a V_{BE} of 2.5 volt. Since the E_g of $In_{0.1}Ga_{0.9}As$ (1.31 eV) is larger than that of $In_{0.03}Ga_{0.97}As_{0.99}N_{0.01}$ (1.2 eV), the ΔE_c barrier at graded B-C junction is reduced but not completely eliminated. Therefore, β and V_{on} of graded B-C junction DHBTs are slightly improved. To effectively eliminate the effect of ΔE_c barrier at the B-C junction on β, indium composition ramping up from 0 to 0.2 in the graded

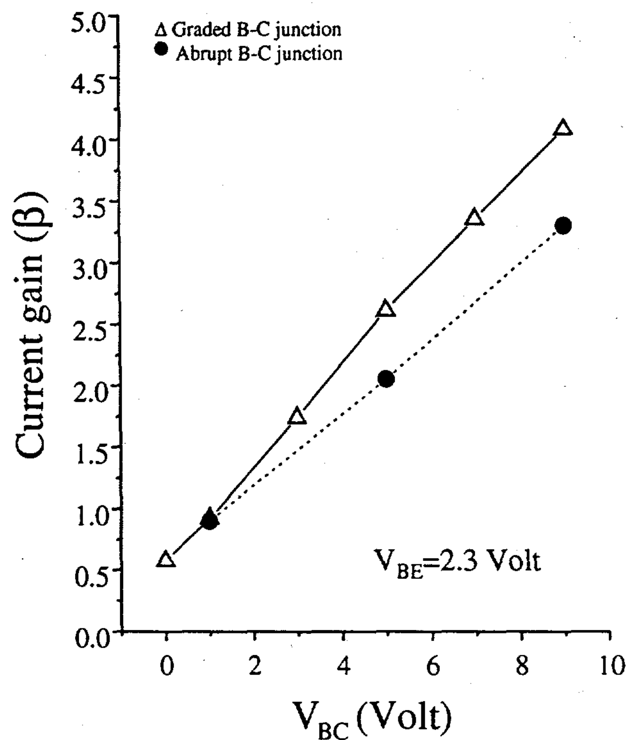

Figure 5: β as a function of V_{BC} for abrupt and graded B-C junction Npn InGaAsN DHBTs with V_{BE}=2.3 volt

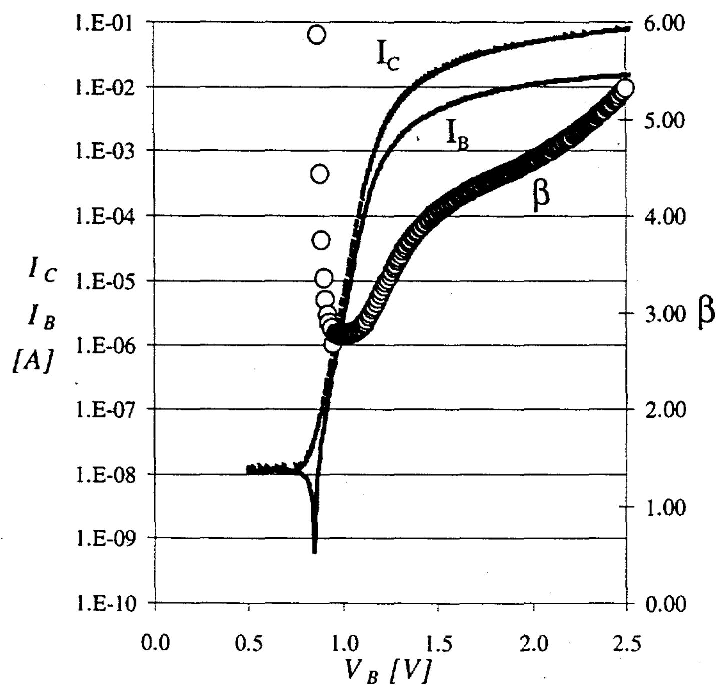

Figure 6: The Gummel plot of an Npn InGaP/InGaAsN DHBT with V_{BC}=9 volt

layer with an n-type δ-doping sandwiched at the B-C junction is studied and listed in Table 3. δ-doping in the emitter near the BE junction has also been inserted to minimize the effect of ΔE_C on the V_{ON}. Two designs for the BC junction have been considered to understand the effect of ΔE_C on the transport of electrons at this junction. The first design (device 1) has an abrupt BC junction, where the ΔE_C is about 0.2 eV. To reduce this barrier, the second design (device 2) uses a strained InGaAs grading layer to gradually increase the E_C from the level of $In_xGa_{1-x}As$ to that of GaAs. The In composition of InGaAs needs to be 0.26 so that the ΔE_C between it and $In_{0.03}Ga_{0.97}As_{0.99}N_{0.01}$ would become zero. However, to avoid strain relaxation effects, the In composition in this structure is limited to 0.20. The In composition grading is linear over a thickness of 30 nm. The $In_{0.2}Ga_{0.8}As$ leaves a ΔE_C of about 0.05 eV at the BC junction, thus a δ-doping layer is inserted in the collector near the BC junction to further improve the transport characteristics of electrons across this interface.

	Device 1			**Device 2**		
Layer	Material	Thickness	Doping	Material	Thickness	Doping
Emitter	n^+ $In_{0.5}GaAs$	300 Å	2×10^{19} cm^{-3}			
	n^+ $In_{0-0.5}GaAs$	300 Å	2×10^{19} cm^{-3}			
	n^+ GaAs	1000 Å	2×10^{18} cm^{-3}	Same as Device 1		
	n InGaP	450 Å	7×10^{17} cm^{-3}			
	InGaP	0 Å	5×10^{12} cm^{-2}			
	n InGaP	50 Å	7×10^{17} cm^{-3}			
Base	p^+ InGaAsN	700 Å	1×10^{19} cm^{-3}	Same as Device 1		
Grading	None			n^- $In_{0.15-0.2}GaAs$	50 Å	3×10^{16} cm^{-3}
				n^- $In_{0.15}$ GaAs	0 Å	5×10^{12} cm^{-2}
				n^- $In_{0-0.15}GaAs$	250 Å	3×10^{16} cm^{-3}
Collector	n^- GaAs	5000 Å	3×10^{16} cm^{-3}	Same as Device 1		
Sub-Coll.	n^+ GaAs	5000 Å	5×10^{18} cm^{-3}	Same as Device 1		
S. I. GaAs Substrate						

Table 3 : Two Npn $InGaP/In_{0.03}Ga_{0.97}As_{0.99}N_{0.01}/GaAs$ DHBTs structures: Device 1 uses an abrupt InGaAsN/GaAs BC junction. Graded InGaAs and δ-doping are introduced in device 2 to improve the carrier transport across the BC junction.

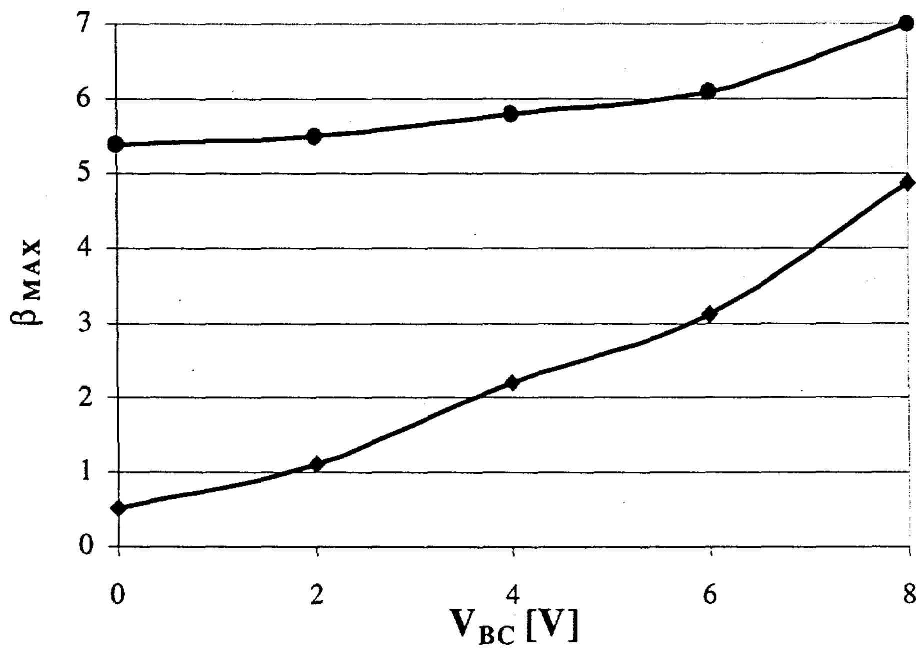

(a)

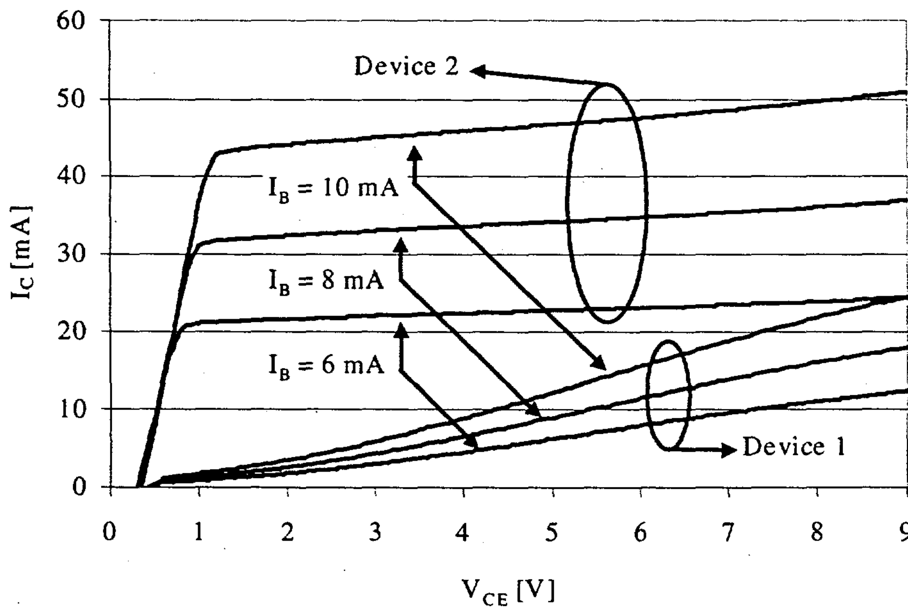

(b)

Figure 7 : (a) The β of the two Npn InGaP/$In_{0.03}Ga_{0.97}As_{0.99}N_{0.01}$/GaAs DHBTs plotted as function of V_{BC} (b) The CE IV plot of the two Npn InGaP/$In_{0.03}Ga_{0.97}As_{0.99}N_{0.01}$/GaAs DHBTs.

The β of the two DHBTs as a function of V_{BC} is shown in Fig. 7a. The β of these devices increase with increasing V_{BC}, especially in the case of device 1, which has an abrupt BC junction. The β of device 1 increases from 0.5 to 4.9 as V_{BC} is increased from 0 to 8 V. The abrupt BC junction of device 1 hinders the electron flow from a quick exit into the collector, and β decreases to less than 1 at zero V_{BC} due to high level of recombination. As V_{BC} increases, the current blocking barrier is lowered, and β increases. In contrast, the β of device 2 is much less dependent, increasing from 5.4 to 7.0 under the same range of V_{BC}. The In composition grading and δ-doping at the BC junction of device 2 has improved the β at zero V_{BC} by more than 10-fold, from 0.52 to 5.4. The CE IV characteristics of both devices are shown in Fig. 7b. Device 2 has nearly ideal IV characteristics compared to the IV characteristics of device 1.

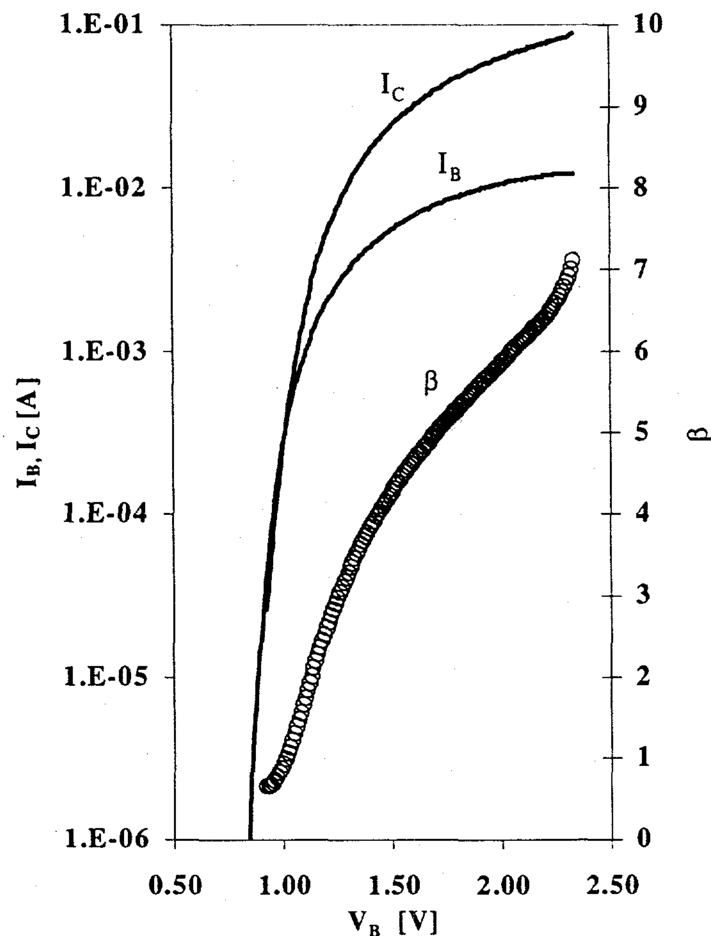

Figure 8 : The Gummel plot of the Npn InGaP/$In_{0.03}Ga_{0.97}As_{0.99}N_{0.01}$/GaAs DHBT under 8 V of BC reverse bias.

The Gummel plot of device 2 at V_{BC} of 8 V is shown in Fig. 8. The ideality factor of I_B and I_C are 1.10 and 1.08, respectively, indicating high-quality InGaP/InGaAsN BE and InGaAsN/GaAs BC junctions. The V_{ON} of device 2 is 0.84 V, which is 0.13 V lower than the 0.97 V measured in an InGaP/GaAs HBT. Even more promising is the lower base current turn on voltage (V_{ONB}). The V_{ONB} of device 2 is only 0.81 V, which is 0.26 V lower than the 1.07 V measured in an InGaP/GaAs HBT. The lower V_{ON} is a strong evidence that HBTs with an InGaAsN base layer has potential to be an alternate approach for reducing power dissipation in a low-power circuit. Also, because GaAs is used for the collector layer, the BV_{CEO} is about 10 V, comparable to the BV_{CEO} observed in an InGaP/GaAs HBT with similar collector thickness and doping level.

The V_{offset} of device 2 is about 220 mV, higher than what is measured in an InGaP/GaAs HBT. The V_{sat} is also slightly higher than in the case of InGaP/GaAs HBT, for I_C of 3 mA, the V_{sat} is about 490 mV. This discrepancy probably arises from the R_B being high. The hole mobility (μ_p) of the InGaAsN in the base layer is about 90 $cm^2V^{-1}s^{-1}$, comparable to the μ_p in GaAs with comparable doping. However, the base doping in our devices is ~1×10^{19} cm^{-3}, lower than the typical base doping of 4-5×10^{19} cm^{-3} used in InGaP/GaAs HBTs. Thus, for a base layer thickness of 70 nm, the R_B is about 1.2 KΩ/Square, about 4 times higher than in a typical InGaP/GaAs HBT. Higher base doping in Npn InGaAsN HBTs would further improve the characteristics of device 2.

Conclusions

In summary, operational Pnp and Npn InGaAsN DHBTs have been demonstrated for the first time. The near ideal band alignment between InGaAsN and GaAs results in near ideal IV characteristics without resorting to grading or delta doping schemes needed in typical Pnp InGaAsN DHBTs. The Pnp InGaAsN DHBT has a peak β of 25. The use of InGaAs grading layer and δ-doping at the BC junction of Npn InGaAsN DHBTs results in near ideal IV characteristics. The Npn InGaAsN DHBT has a peak β of 7. Since the collector is made of GaAs for both Pnp and Npn InGaAsN DHBTs, the BV_{CEO} of Pnp and Npn InGaAsN DHBTs are 12 and 10 V, respectively, comparable to the BV_{CEO} observed in Pnp and Npn GaAs HBTs with similar collector thickness and doping. The 1.2 eV InGaAsN has led to the low V_{ON} of 0.79 and 0.84 V for Pnp and Npn InGaAsN DHBTs, respectively, demonstrating great potential for application of InGaAsN in low-power electronics. Further improvements on the InGaAsN material are still necessary to reduce R_B and improve β, so that the full potential of InGaAsN for low-power applications can be realized.

Sandia is a multiprogram laboratory operated by Sandia Corporation, a Lockheed Martin Company, for the United States Department of Energy under Contract DE-AC04-94AL85000.

Reference

[1] S. M. Sze, High-speed Semiconductor Devices (John Wiley & Sons Inc, New York, 1990) ch6, p358.
[2] S. Sakai, Y. Ueta, and Y. Terauchi, Jpn. J. Appl. Phys., 32 (1993) 4413.
[3] J. A. Van Vechten, Phys. Rev., 182 (1969) 891.
[4] S. Sato, and S. Satoh, Electron. Lett., 35 (1999) 1251.
[5] N. Y. Li, C. P. Hains, K. Yang, J. Lu, J. Cheng, and P. W. Li, Appl. Phys. Lett., 75 (1999) 1051.
[6] S. R. Kurtz, A. A. Allerman, E. D. Jones, J. M. Gee, J. J. Banas, Appl. Phys. Lett., 74 (1999) 729.
[7] H. P. Xin, C. W. Tu, and M. Geva, Appl. Phys. Lett., 75 (1999) 1416.
[8] N. Y. Li, P. C. Chang, A. G. Baca, X. M. Xie, P. R. Sharps, and H. Q. Hou, Electron. Lett., 36 (2000) 81.
[9] P. C. Chang, A. G. Baca, N. Y. Li, P. R. Sharps, H. Q. Hou, J. R. Laroche, and F. Ren, Appl. Phys. Lett., 76 (2000) 2262.
[10] M. Kondow, K. Uomi, A. Niwa, T. Kitatani, S. Watahiki, and y. Yazawa, Jpn. J. Appl. Phys., 35 (1996) 1273.
[11] L. C. Wang, P. H. Hao, and B. J. Wu, Appl. Phys. Lett., 67 (1995) 509.